
This is an electronic reprint of the original article.
This reprint may differ from the original in pagination and typographic detail.

Jávor, Z.; Schreithofer, N.; Heiskanen, K.

Kernel functions to flotation bubble size distributions

Published in:
Minerals Engineering

DOI:
[10.1016/j.mineng.2018.05.012](https://doi.org/10.1016/j.mineng.2018.05.012)

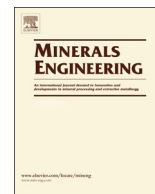
Published: 15/08/2018

Document Version
Publisher's PDF, also known as Version of record

Published under the following license:
CC BY-NC-ND

Please cite the original version:
Jávor, Z., Schreithofer, N., & Heiskanen, K. (2018). Kernel functions to flotation bubble size distributions. *Minerals Engineering*, 125, 200-205. <https://doi.org/10.1016/j.mineng.2018.05.012>

This material is protected by copyright and other intellectual property rights, and duplication or sale of all or part of any of the repository collections is not permitted, except that material may be duplicated by you for your research use or educational purposes in electronic or print form. You must obtain permission for any other use. Electronic or print copies may not be offered, whether for sale or otherwise to anyone who is not an authorised user.



Kernel functions to flotation bubble size distributions

Z. Jávora^a, N. Schreithofer^{b,*}, K. Heiskanen^c

^a Université de Lorraine, GeoRessources, CNRS, UMR 7359, 2 rue du Doyen Marcel Roubault, TSA 70605, France

^b Department of Bioproducts and Biosystems, School of Chemical Engineering, Aalto University, Finland

^c Department of Chemical and Metallurgical Engineering, School of Chemical Engineering, Aalto University, Finland



ARTICLE INFO

Keywords:

Flotation modelling
Bubble size
Bubble breakage
Bubble coalescence
CFD
PBM
Frothers

ABSTRACT

Flotation modelling has advanced from deterministic single particle-bubble models into using such models to solve flotation systems by using modern computational techniques. The step from a single particle- single bubble event to multiple events taking place in the large computational volume like a flotation cell poses the challenge of handling bubble and particle distributions in all computational cells.

The estimation of bubble size has either been omitted (constant size) or has been lately estimated by a population balance approach. The physical performance of flotation is excessively determined by the bubble size distribution (BSD). Therefore, the bubble size distribution estimate is crucial for modelling. Although the BSD can be measured, the underlying effects of different variables causing changes in break-up and coalescence rates producing changes in the measured BSD's are not well understood. This paper discusses the profound effects frothers have on both the coalescence and break-up of gas bubbles.

Depending on the bubble surface stiffness caused by frother adsorption, the drainage rate of fluid between two approaching bubbles is very different. Frothers like DF200 and Pentanol have a higher coalescence rate than frothers like DF250 and NF240.

Break-up is shown to be a function of the dynamic surface tension, not the static surface tension. Fast adsorbing frothers (DF200) have at very short time scales a higher rate of break-up.

The paper suggests a division of frothers into two distinct classes for modelling purposes. Those with fast adsorption and desorption, which leave the gas-air interface mobile and those frothers that by slower adsorption and desorption create stiff interfaces. The effects in real systems may be more varied. The modelling of subtler frother effects will not substantially improve modelling quality.

1. Introduction

Flotation modelling has the challenge to combine several physico-chemical phenomena into a concise model framework. The main body of modelling has been related to the well-known first order reaction model. During the years this approach with its additions and improvements has proven to be a good simple engineering model to be fitted with batch flotation data results *e.g.* a plug flow reactor.

$$\frac{dC}{dt} = -kC. \quad (1)$$

The rate constant k can be obtained experimentally for any given steady-state condition. However, to formulate the dependence of the rate constant from process variables has turned out to be difficult. There have been attempts to relate the rate constant to both local and global parameters (Jameson *et al.*, 1977) and to link the rate constant to the probabilistic bubble-particle encountering by the time averaged bubble

horizontal interface flux (termed bubble surface area flux S_b) (Gorain *et al.*, 1995a,b, 1996, 1999). To make the challenge more tractable, the total process has been generally divided into probabilistic sub-processes as outlined first by Gaudin (1932) and in more detail by Sutherland (1948). The “total probability of flotation” consists of the sub-process probabilities *e.g.* particle-bubble collision, attachment and stability (detachment)

$$k = P_f S_b. \quad (2)$$

The flotation rate k is then modelled as a product of the “total probability of flotation” and the frequency that bubbles and particles interact (come so close to each other for the above mentioned sub-processes to take place *e.g.* collide).

$$ZP_f = ZP_c P_a P_s = k. \quad (3)$$

There are several deterministic models for the particle-bubble collision (Gaudin, 1932; Sutherland, 1948; Yoon and Luttrell, 1989;

* Corresponding author.

E-mail addresses: zoltan-lajos.javor@univ-lorraine.fr (Z. Jávora), nora.schreithofer@aalto.fi (N. Schreithofer), kari.heiskanen@outotec.com (K. Heiskanen).

Langmuir, 1948; Flint and Howarth, 1971; Dukhin, 1982; Dai et al., 2000). All these models, not repeated here, are considering a single bubble-particle pair. All of them show in general a relation between the collision frequency, particle (p) and bubble size (b) as

$$E_c = A \left(\frac{p}{b} \right)^n, \quad (4)$$

where parameter A varies from 3/2 in laminar to 3 in potential flows and n from 2 to 1, respectively.

A challenge has been how to expand the single bubble-particle pair models to handle large interacting bubble and particle populations.

Computational Fluid Dynamics (CFD) has become a versatile and indispensable tool to model any fluid flows containing devices and equipment, flotation devices among them. The challenges for meaningful flotation CFD are several, as the aim is to model two discrete poly-disperse phases interacting in a continuous fluid phase. Without discussing and detailing them, an important question to be asked is “What is the bubble size to be used in flotation modelling?”

A hypothesis to estimate bubble size has been to define a critical concentration from where added frother has no further effect on bubble coalescence (coalescence is prevented) and a minimum bubble size is reached (Cho and Laskowski, 2002). The minimum bubble size (b_0) is attributed to machine design and operation parameters but many authors highlighted that the minimum bubble size is also affected by frother type as it can influence the bubble break-up mechanism caused by turbulent eddies in high intensity zone (Chu et al., 2016; Jávora et al., 2013, 2016; Kracht and Finch, 2009). In industrial measurements of bubble size distributions Nasset et al. (2007) found cases with substantially differing distributions. Coalescence prevention as a determining factor of bubble size in flotation machines was questioned by Finch et al. (2008) using the data from the study of Nasset et al. (2007). However, the properties of the air/liquid interface are substantially determined by the rheological properties of the adsorbed layers (Fruhner et al., 1999) indicating possibilities of both bubble coalescence and break-up.

Population balance models (PBM) can be used in conjunction with CFD to estimate the local poly-disperse phase distributions, here the bubble number density functions (NDF) (Bhutani, 2016). The PBM conservation equation is

$$\frac{\partial n(b,x,t)}{\partial t} + \nabla \cdot ((ub)n) - \nabla \cdot (\bar{D}_x(b,x,t) \nabla n) = S_b(b,x,t), \quad (5)$$

where $n(b,x,t)$ is the number density function, b is the internal (bubble property, e.g. size) and x the external spatial coordinate respectively. The second and third terms on the left are the advective and diffusive parts of bubbles migrating (external coordinate space). The right-hand term is the source term describing all the processes taking place in the internal coordinate space

$$S_b = B_{br} - D_{br} + B_{co} - D_{co}, \quad (6)$$

where B_{br} and B_{co} are the birth functions due to bubble breakage and coalescence respectively. D_{br} and D_{co} are the respective death functions.

$$B_{br}(b) = \int_{\xi}^{\infty} m(b_1) a(b_1) c(b|b_1) n(b_1) db_1, \quad (7.1)$$

$$D_{br}(b) = a(b) n(b), \quad (7.2)$$

$$B_{co}(b) = \frac{1}{\delta} \int_0^{\infty} \left(\frac{b^2}{b'^2} \right) \beta(b', b_1) n(b') n(b) db_1, \quad (7.3)$$

$$D_{co}(b) = \int_0^{\infty} \beta(b, b_1) n(b) n(b_1) db_1. \quad (7.4)$$

Bubble breakage kernels $m(b_1)$, $a(b_1)$ and $c(b|b_1)$ define the number of bubbles produced in a break-up event, the frequency of break-up and the daughter distribution function respectively. Kernel $\beta(b|b_1)$ is the coalescence event frequency. This has also been divided into two parts, collision frequency and collision efficiency.

Population balance models can be solved either by the method of classes, where the NDF is discretized into a number of classes. Each class leads to an equation considering all the processes that will affect the units of the said class. The issue rising is mainly the bubble breakage and bubble coalescence. Each class would need its own kernel functions. The benefit is the natural reconstruct of the NDF. It is, however, computationally very expensive and time consuming to be used in flotation simulation. The other method to solve the bubble PBM is the method of quadrature of moments (QMOM) (McGraw, 1997; Marchisio and Fox, 2005; Bhutani, 2016). In the method the moments of the NDF are solved from the available transported moments. As is discussed by Bhutani (2016), for an approximate estimate of NDF four moments is often sufficient. For this approach a set of kernel functions would be sufficient. This, however, requires robust kernels.

Bubble break-up and coalescence kernels have been studied extensively for bubble columns (Prince and Blanch, 1990a; Luo and Svendsen, 1996; Martinez-Bazan et al., 1999, 2010; Lehr and Mewes, 2001; Wang et al., 2003; Zhao and Ge, 2007; Liao and Lucas, 2009, 2010; Solsvik and Jakobsen, 2015 among others). These studies have performed with electrolytes. They differ in several important aspects from flotation systems with varying chain length surface active reagents (frothers) and solids.

2. Bubble break-up kernels

The Martinez-Bazan et al. (2010) model assumes that a pair of bubbles can be formed, when the stresses caused by turbulence are larger than the stresses opposing deformation at the length scales corresponding to the mother bubble. There exists always a critical bubble size at each level of turbulent intensity that cannot be broken up. This critical size is expressed as

$$b_{crit} = \varepsilon^{-2/5} \left(\frac{12\lambda}{\beta\rho_s} \right)^{3/5}, \quad (8)$$

where ε is the turbulent energy dissipation, λ_s surface tension (without surfactant), ρ the density and β a constant. The probability of break-up is (Martinez-Bazan et al., 2010) for a bubble with a volume V is as follows

$$P_V(V^*) \propto \left(\frac{1}{2} \rho \beta (\varepsilon b_0)^{2/3} \right)^2 (V^{*2/9} - \Lambda^{5/3}) ((1-V^*)^{2/9} - \Lambda^{5/3}), \quad (9)$$

where b_0 is the mother bubble diameter, V its volume and Λ the ratio between the mother bubble size b_0 and the critical bubble size b_{crit} . The obtained bubble size distribution is (Martinez-Bazan et al., 2010):

$$f^*(b^*) = \frac{b^{*2} [b^{*2/3} - \Lambda^{5/3}] [(1-b^{*3})^{2/9} - \Lambda^{5/3}]}{\int_{b_{min}^*}^{b_{max}^*} b^{*2} [b^{*2/3} - \Lambda^{5/3}] [(1-b^{*3})^{2/9} - \Lambda^{5/3}] db^*}. \quad (10)$$

If surfactants are added to the solution in dilute concentrations their adsorption on the gas-water interphase will change the surface tension in a linear way

$$\lambda_s - \lambda = \Gamma^* R T, \quad (11)$$

where λ_s is the surface tension without the surfactant. Γ^* is the surface concentration of the surfactant (mass of surfactant per unit area of surface). Following the linear relationship, one can write for a small change in the surfactant to have an effect on the surface tension as follows (Stone and Leal, 1990)

$$\lambda^* - \lambda_s = (1 - \varphi). \quad (12)$$

This will change the critical bubble size of Eq. (8) to

$$b_{crit} = \varepsilon^{-2/5} \left(\frac{12\lambda_s(1-\varphi)}{\beta\rho} \right)^{3/5}. \quad (13)$$

As Martinez-Bazan et al. (2010) point out, the parameter Λ in Eq.

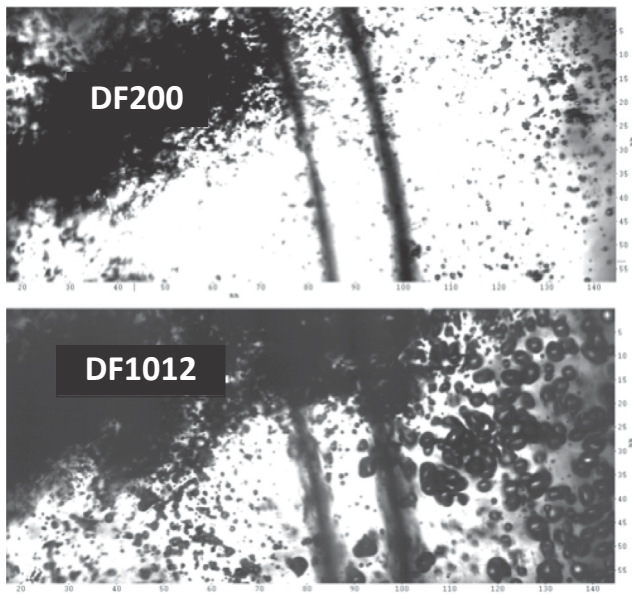


Fig. 1. High speed snapshots from a 300 mm Outotec “freeflow” rotor at 20 ppm DF 200 and DF1012 frother concentrations. (water only). Pictures taken through the bottom of the flotation cell into from upwards direction. Courtesy Juha Tiitinen (unpublished).

(9) can be interpreted as the inverse of the mother bubble Weber number

$$We = \frac{\rho\beta\epsilon^{2/3}b_0^{5/3}}{12\lambda^*} \tag{14}$$

The critical Weber number is given as 2.2 for this model (Martinez-Bazan et al., 1999). The Weber number will decrease also with a factor (1 - φ).

Grau et al. (2005) measured the surface tensions at very low concentrations in equilibrium conditions showing the expected larger decrease in surface tension of “stronger” frothers DF250 and DF1012 and a much lower decrease with DF200 (Fig. 11 of Grau et al.). However high-speed photos taken from outside of a 300 mm impeller indicate that the bubble size at the rotor is much finer with the DF200 (Fig. 1).

Jávor (2014) showed the need to use dynamic surface tension values in evaluating the correction factor in Eq. (13) instead of static values (Fig. 2). Of the different frothers tested DF200 decreased the critical bubble size with about 10%, while the “stronger” frothers NF240 and DF 250 had only a marginal 2–3% decrease at very short bubble lifetimes. What is to be noted is the temporal change in NF 240

and 250 frothers. As bubbles age, the critical bubble size starts to decrease. As an outcome in a flotation cell is that after the imminent breakage of the bubbles close to the impeller, the probability of further bubble breakage diminishes rapidly. This indicates that bubble breakage kernels of the source term (Eq. (5)) need to be used only in cases, where the critical bubble size is above the limit in Eq. (13). The results of Jávor (2014) indicate that the assumption for the velocity field to be independent from the internal coordinates (Eq. (5)) may not hold. There are also indications that in a turbulent field the inertia of attached bubbles creates additional breakage mechanisms (Omelka et al., 2009).

3. Bubble coalescence kernels

In pure water gas bubbles have a tendency to coalesce as has been observed in flotation systems by Finch et al. (2008). Bubble coalescence takes place in three steps (Prince and Blanch, 1990a). Bubbles need to collide (e.g. come close enough for liquid to get trapped between the bubbles). In the second phase the liquid drains away until it reaches a critical thickness. As that thickness is reached the van der Waals forces cause the film to break. There is a large body of literature discussing bubble coalescence (Marrucci and Nicodemo, 1967; Sagert et al., 1976; Derjaguin and Churaev, 1978; Prince and Blanch, 1990b; Marrucci, 1969; Craig et al., 1993a, 1993b; Christenson and Yaminsky, 1995; Deschenes et al., 1998; Marcelja, 2006; Henry et al., 2007; Christenson et al., 2008; del Castillo et al., 2011 and others). In a simplified model we can multiply the collision rate with a success rate (Eq. (15)) in order to get a coalescence birth kernel for CFD modelling.

The simple equation for coalescence success rate Coualoglou (1975) suggested is

$$p_c(b, b_1) = \text{Exp}\left(-\frac{t_{\text{drainage}}}{t_{\text{contact}}}\right) \tag{15}$$

It relates the time the bubbles spend at a distance where the drainage of the film takes place (t_{contact}) to the time it takes for the film drain to a thickness where van der Waals forces rupture the thinned film (t_{drainage}). Machon et al. (1997) added a boundary condition

$$p_c = 0, \text{ if } t_{\text{drainage}} < t_{\text{contact}} \tag{15b}$$

The drainage is governed by the following equations (Chesters and Hofman, 1982; Carnie et al., 2005), where p is hydrodynamic pressure, Π disjoining pressure, λ surface tension and μ dynamic viscosity (see notations in Fig. 3).

$$\Delta p - (p + \Pi) = \frac{\lambda}{r} \left(r \frac{\partial h}{\partial r} \right) \tag{16}$$

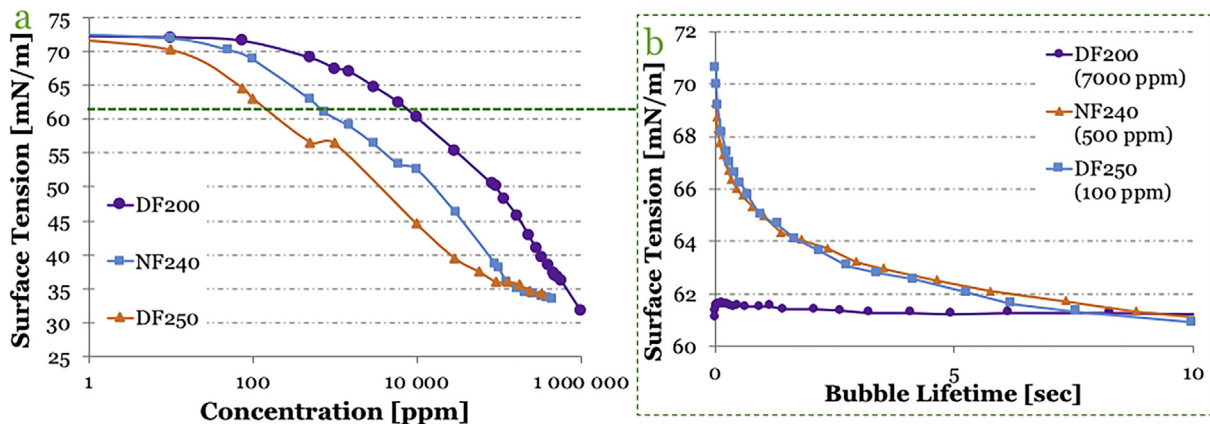


Fig. 2. (a) Static surface tension as a function of frother concentration and (b) dynamic surface tension at equivalent static surface tension (61 mN/m) concentration (Jávor, 2014).

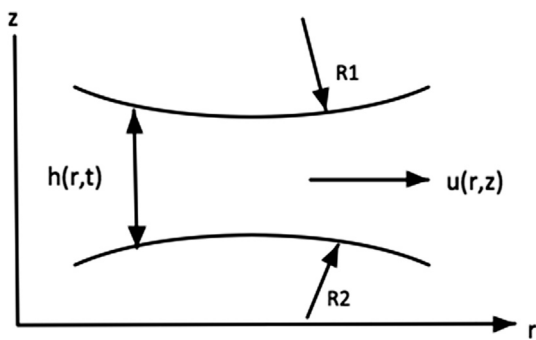


Fig. 3. The notations for Eqs. (16)–(18).

$$\frac{\partial h}{\partial r} = \frac{1}{r} \frac{\partial}{\partial r} \left[r \int_0^{h(r,t)} u(z,t) dz \right], \tag{17}$$

$$u \frac{\partial^2 u}{\partial z^2} = \frac{\partial p}{\partial r}. \tag{18}$$

If the bubble surface is immobile then $u(z,r)_{z=h} = 0$ and the result is a parabolic Poiseuille flow

$$\frac{\partial h}{\partial t} = \frac{1}{12\mu r} \frac{\partial}{\partial r} \left(rh^3 \frac{\partial p}{\partial r} \right). \tag{19}$$

For a fully mobile surface $u(z,r)_{z=h} \neq 0$ leads to a boundary condition of $\partial u / \partial z = 0$. The final outcome is a plug flow profile with a four times faster rate of bubble distance (h) diminishing.

$$\frac{\partial h}{\partial t} = \frac{1}{3\mu r} \frac{\partial}{\partial r} \left(rh^3 \frac{\partial p}{\partial r} \right). \tag{20}$$

The real situation is more complex due to surfactant concentration gradients and resulting Marangoni stresses. However, such details are not rate determining in flotation CFD modeling (Finch et al., 2008). As a first estimate we can use viscoelasticity to define the flow regime (Fig. 4). The surface active frothers DF250 and PPG425 show marked viscoelasticity, while DF200 and 1-Pentanol had viscoelasticity values below the detection limit (dilatation elasticity method was employed for viscoelasticity measurement that has a relatively low reproducibility in test solutions where the measured viscoelasticity does not rise above 1.5 mN/m). For DF250 and PPG425 Eq. (19) should be used and for DF200 and 1-Pentanol Eq. (20) is to be used.

If Eqs. (19) and (20) are taken to represent the different frothers depending on their viscoelastic behavior and their drainage rate we can see in Fig. 5 a very marked difference in the relative coalescence rates computed using the Coualaloglou equation (Eq. (15)).

Horn et al. (2011) have mapped the effects of bubble approach

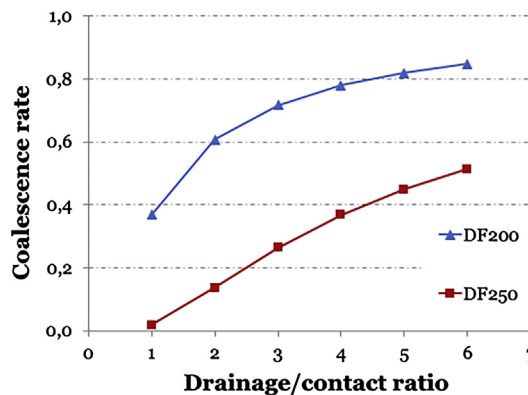


Fig. 5. Difference in coalescence rates.

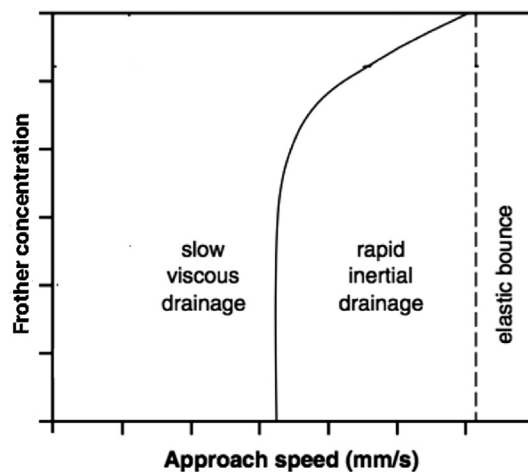


Fig. 6. A partial reproduction of the Fig. 2 (Horn et al., 2011) with the Yaminsky critical approach velocity (Eq. (21)) (Yaminsky et al., 2010).

velocity and NaCl concentrations on coalescence (Partially reproduced as Fig. 6). Fig. 6 is intentionally left without axis values; as such data for commercial frothers is not available. The slow viscous drainage represents the immobile frother surfaces (DF250 and PPF 425) and the rapid inertial drainage represents the mobile surfaces (DF200 and 1-Pentanol). The study of Horn et al. (2011) indicate that there exists a critical speed of approach V_c , which has an impact on the relative immobility of the surfaces (Yaminsky et al., 2010).

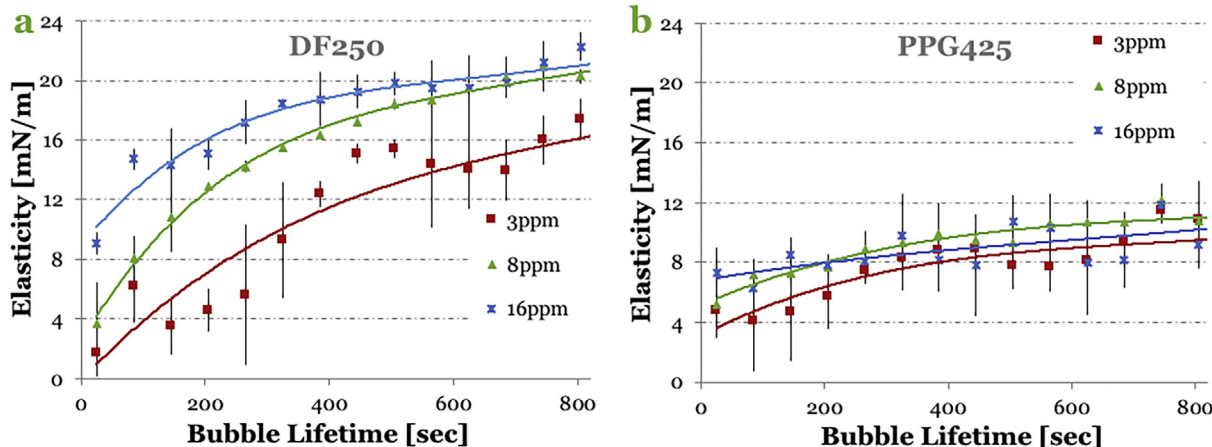


Fig. 4. Viscoelasticity of DF250 and PPG425 (Jávora, 2014).

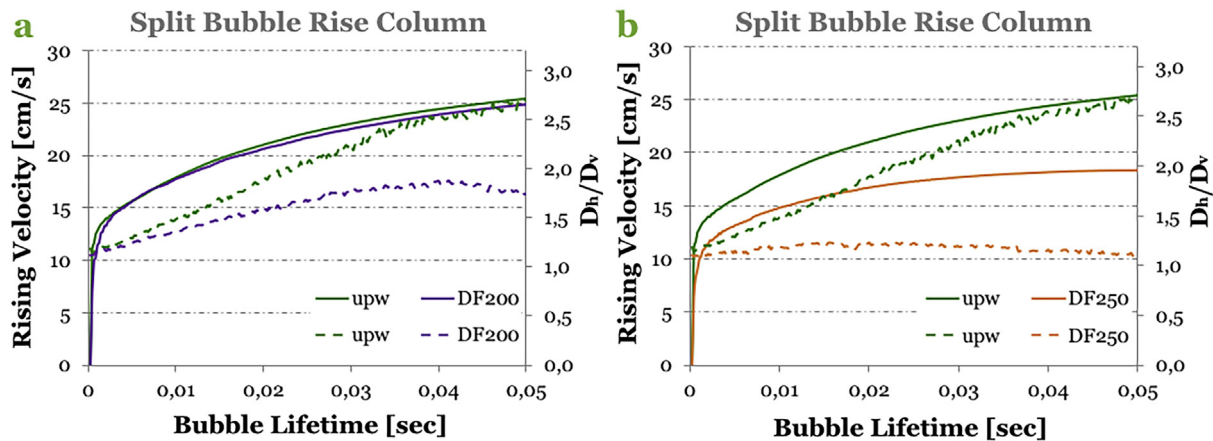


Fig. 7. Rising velocity (solid line) and aspect ratio (dashed line) of the bubble observed in SBRC [In split bubble rise column (SBRC) the bubbles were released to the lower part of the column containing ultrapure water and directed by a valve to the upper part filled with surfactant solution.] (a) in 8 ppm DF200; (b) in 8 ppm of DF250 (upw denotes ultra-pure water) (Jávora, 2014).

$$V_c = \left(\frac{4}{3}\right)^3 \frac{(\Delta\gamma)^2}{\gamma} \frac{1}{\mu}, \quad (21)$$

where $\Delta\gamma$ is the surface tension gradient from the bubble centreline outwards. The equation does not take into consideration the different behaviour of frothers, like their effects on surface viscoelasticity. The equation, however, indicates the existence of a critical bubble approach velocity as also has been considered by Kirkpatrick and Lockett (1974).

As surfactants are adsorbed onto the surface the increased rigidity of the surfaces decreases the velocity difference between the fluid and the bubble substantially. Clift et al. (1978) showed (their Fig. 7.3) in compiling the results from several researchers that for one and two millimetre bubbles the terminal velocity difference can be in uncontaminated systems over 10 cm/s and in contaminated rigid systems 5–6 cm/s. Jávora (2014) showed that different frothers had marked effects on bubble rise velocity (Fig. 7). The less surface active DF200 (Fig. 7a) has less pronounced effect on the interface rigidity (defined by the aspect ratio of the bubble – secondary y-axes) compared to the ultra-pure water (upw) therefore the rising velocity data does not suggest any change in rising velocity. Whereas the more surface-active agent (Fig. 7b) made the interface rigid within milliseconds reducing rising velocity significantly within a short period of time.

There are three different mechanisms for bubbles to collide. The first is due to turbulent fluctuations. Prince and Blanch (1990a) give for that probability

$$P_{coT} = \frac{\pi}{2\sqrt{2}} (b_1 + b_2)^2 e^{1/3} (b_1^{2/3} + b_2^{2/3})^{1/3}. \quad (22)$$

The second is due to buoyancy induced velocity differences. Liao et al. (2015) gives

$$P_{cobu} = 0.5 \frac{\pi}{4} (b_1 + b_2) |v_{b1} - v_{b2}|. \quad (23)$$

The third mechanism is by viscous shear close to the impeller. Liao et al. (2015) gives

$$P_{covis} = 0.5 \frac{\pi}{4} (b_1 + b_2)^2 \left[0.5 \frac{\pi}{4} (b_1 + b_2) \gamma_f \right]. \quad (24)$$

Summing up these will give the total collision probability.

$$P_{Co} = P_{coT} + P_{cobu} + P_{covis}. \quad (25)$$

The first mechanism is only related to bubble sizes and the turbulent energy dissipation. Eq. (22) assumes that bubbles take the velocity of an equal size eddy. However small eddies do not contain sufficient energy to affect bubble motion and large eddies do not generate much relative motion. Omelka et al. (2009) showed that the slide of particles on the surface of a bubble retard bubble movement in an eddy. The second

mechanism is based on the assumption of a relative velocity maintained within the bubbles. Eq. (25) may not capture the physical complexity of bubble-bubble collisions to a degree sufficient for modelling.

We can write the coalescence kernel (Eq. (7.3)) by combining Eqs. (15) and (25) to get

$$\beta(b, b_1) = P_{Co} p_c(b, b_1) = P_{Co} \text{Exp}(-\alpha \xi_p(V, b, b_1)), \quad (26)$$

where $\alpha = 1$ for mobile surfaces and $\alpha = 4$ for immobile surfaces, $\xi(V, b, b_1)$ the ratio between drainage time and contact time in a pure system at an approach velocity V .

4. Discussion

Computational modelling of flotation has drawn much of its methods and algorithms from the works dealing with bubbly flows (e.g. Lehr and Mewes, 2001; Marchisio and Fox, 2005; McGraw, 1997; Marrucci, 1969 and several others). These models have used information of bubble behaviour from experimental work done in electrolyte systems (e.g. Liao and Lucas, 2010; Yaminsky et al., 2010; Horn et al., 2011). Frothers are different in several aspects from electrolytes. The basic difference is that frothers are adsorbed onto the surface and change the surface “stiffness” as discussed above. The hysteresis between adsorption and desorption in a flow field is one of the most important features (Jávora, 2014) differentiating the frother effects from electrolyte effects.

The film drainage model used in computational modelling determines the coalescence efficiency (and therefore the bubble size distribution) from the characteristic time scales of surface contact and drainage. The former is strongly determined by fluid dynamic while the latter is by bubble surface rigidity (Lee and Hodgson, 1968). By linking the bubble surface mobility to characterisable surface property that can be easily measured in dynamic water-surfactant solution can help to get a step closer to a physical based model. The above presented approach is an attempt of integrating frother properties into the modelling that could bring more realistic bubble size distributions estimates.

5. Conclusions

The direct use of kernel equations derived from pure systems or from studies performed with electrolytes (notably NaCl) lead to wrong estimates of the bubble size at any spatial volume modelled. The characteristics of frothers have not been taken into consideration in the modelling of bubble behaviour. For bubble break-up it is proposed to take the frother effects into account by a correction factor dependent on the dynamic surface tension (Eqs. (12) and (13)). It is argued that

break-up kernel computations are really needed only at volumes with high turbulent energy dissipation.

It has been shown that frothers can be divided into two major categories (for modelling purposes) based on their effects on viscoelasticity. Frothers like DF200 will have a coalescence drainage behaviour best described by a plug flow of liquid, while frothers like DF250 produce a parabolic Poiseuille flow. This difference in behaviour can be simplified to be taken into account in the coalescence kernel only by a constant factor of four (Eq. (26)). It is acknowledged that there exists a critical bubble-bubble approach velocity, but equations derived for pure systems do not capture the phenomena taking place in flotation in such a way that they could be used in developing the kernel models.

As a simplified outcome for flotation CFD modelling, we propose two modelling regimes depending on the properties of the used frother for the time being.

For future improvements of flotation modelling more frother behaviour derived data is needed to “fill” the framework presented as Fig. 6 (Horn et al., 2011; Yaminsky et al., 2010).

References

- Bhutani, G., 2016. Numerical Modelling of Polydispersed Flows Using an Adaptive Mesh Finite Element Method with Application to Froth Flotation. Doctoral Thesis. Imperial College, London.
- Carnie, S.L., Chan, D.Y.C., Lewis, C., Manica, R., Dagastine, R.R., 2005. Measurement of dynamical forces between deformable drops using the atomic force microscope. *I. Theory*. *Langmuir* 21, 2912–2922.
- Chesters, A.K., Hofman, G., 1982. Bubble coalescence in pure liquids. *Appl. Sci. Res.* 38, 353–361.
- Cho, Y.S., Laskowski, J.S., 2002. Effect of flotation frothers on bubble size and foam stability. *Int. J. Miner. Process.* 64, 69–80.
- Christenson, H.K., Yaminsky, V.V., 1995. Solute effects on bubble coalescence. *J. Phys. Chem.* 99, 10420.
- Christenson, H.K., Bowen, R.E., Carlton, J.A., Denne, J.R.M., Lu, Y., 2008. Electrolytes that show a transition to bubble coalescence inhibition at high concentrations. *J. Phys. Chem. C* 112, 794–796.
- Chu, P., Waters, K.E., Finch, J.A., 2016. Break-up in formation of small bubbles: comparison between low and high frother concentrations. *Miner. Eng.* 96–97, 15–19.
- Clift, R., Grace, J.R., Weber, M.E., 1978. *Bubbles Drops and Particles*. Academic Press.
- Coulaloglou, C.A., 1975. *Dispersed Phase Interactions in an Agitated Flow Vessel*. Ph.D. Dissertation. Illinois Institute of Technology, Chicago.
- Craig, V.S.J., Ninham, B.W., Pashley, R.M., 1993a. Effect of electrolytes on bubble coalescence. *Nature* 364, 317–319.
- Craig, V.S.J., Ninham, B.W., Pashley, R.M., 1993b. The Effect of electrolytes on bubble coalescence in water. *J. Phys. Chem.* 97, 10192–10197.
- Del Castillo, L.A., Ohnishi, S., Horn, R.G., 2011. Inhibition of bubble coalescence: Effects of salt concentration and speed of approach. *J. Colloid Interface Sci.* 356, 316–324.
- Dai, Z., Fornasiero, D., Ralston, J., 2000. Particle/bubble collision models / a review. *Adv. Colloid Interf. Sci.* 85, 231–256.
- Derjaguin, B.V., Churaev, N.V., 1978. On the question of determining the concept of disjoining pressure and its role in the equilibrium and flow of thin films. *J. Colloid Interface Sci.* 66, 389–398.
- Deschenes, L.A., Barrett, J., Muller, L.J., Fourkas, J.T., Mohanty, U., 1998. Inhibition of bubble coalescence in aqueous solutions. 1. Electrolytes. *J. Phys. Chem. B* 102, 5115–5119.
- Dukhin, S., 1982. The role of inertial forces in the flotation of small particles (in Russian). *Colloid J.* 44 (3), 431–441.
- Finch, J.A., Nasset, J.E., Acuña, C., 2008. Role of frother on bubble production and behaviour in flotation. *Miner. Eng.* 21, 949–957.
- Flint, L.R., Howarth, W.J., 1971. The collision efficiency of small particles with spherical air bubbles. *Chem. Eng. Sci.* 26, 155–168.
- Fruhner, H., Wantke, K.-D., Lunkenheimer, K., 1999. Relationship between surface dilatational properties and foam stability. *Colloids Surf. A* 162, 193–202.
- Gaudin, A.M., 1932. *Flotation*. McGraw-Hill, New York.
- Gorain, B.K., Franzidis, J.-P., Manlapig, E.V., 1995a. Studies on impeller type, impeller speed and air flow rate in an industrial scale flotation cell. Part 1. Effect on bubble size distribution. *Miner. Eng.* 8 (6), 615–635.
- Gorain, B.K., Franzidis, J.-P., Manlapig, E.V., 1995b. Studies on impeller type, impeller speed and air flow rate in an industrial scale flotation cell. Part 2. Effect on gas holdup. *Miner. Eng.* 8 (12), 1557–1570.
- Gorain, B.K., Franzidis, J.-P., Manlapig, E.V., 1996. Studies on impeller type, impeller speed and air flow rate in an industrial scale flotation cell. Part 3. Effect on superficial gas velocity. *Miner. Eng.* 9 (6), 639–654.
- Gorain, B.K., Franzidis, J.-P., Manlapig, E.V., 1999. The empirical prediction of bubble surface area flux in mechanical flotation cells from cell design and operating data. *Miner. Eng.* 12 (3), 309–322.
- Grau, R., Laskowski, J., Heiskanen, K., 2005. Effect of frothers on bubble size. *Int. J. Min. Proc.* 75, 225–233.
- Henry, C.L., Dalton, C.N., Scruton, L., Craig, V.S.J., 2007. Ion-specific coalescence of bubbles in mixed electrolyte solutions. *J. Phys. Chem. C* 111, 1015–1023.
- Horn, R.G., Del Castillo, L.A., Ohnishi, S., 2011. Coalescence map for bubbles in surfactant-free aqueous electrolyte solutions. *Adv. Colloid Interface Sci.* 168, 85–92.
- Jávora, Z., 2014. *Frother controlled interfacial phenomena in dynamic systems – holistic approach*. Doctoral Dissertation. Aalto University Publication series Doctoral Dissertations 161/2014.
- Jameson, G.J., Nam, S., Young, M.M., 1977. Physical factors affecting recovery rates in flotation. *Min. Sci. Eng.* 9 (3), 103–118.
- Jávora, Z., Schreithofer, N., Gomez, C.O., Finch, J.A., Heiskanen, K., 2013. Effect of scale dependent dynamic properties on bubble size. In: *Materials Science and Technology Conference and Exhibition 2013, MS and T 2013*.
- Jávora, Z., Schreithofer, N., Heiskanen, K., 2016. Multi-scale analysis of the effect of surfactants on bubble properties. *Miner. Eng.* 99, 170–178.
- Kirkpatrick, R.D., Lockett, M.J., 1974. The influence of approach velocity on bubble coalescence. *Chem. Eng. Sci.* 29, 2363–2373.
- Kracht, W., Finch, J.A., 2009. Bubble break-up and the role of frother and salt. *Int. J. Miner. Process.* 92, 153–161.
- Langmuir, I., 1948. The production of rain by a chain reaction in cumulus clouds at temperature above freezing. *J. Meteorol.* 5 (5), 175–192.
- Lehr, F., Mewes, D., 2001. A transport equation for the interfacial area density bubble columns. *Chem. Eng. Sci.* 56, 1159–1166.
- Lee, J.C., Hodgson, T.D., 1968. Film flow and coalescence – I basic relations film shape and criteria for interface mobility. *Chem. Eng. Sci.* 23, 1375–1397.
- Liao, Y., Lucas, D., 2009. A literature review of theoretical models for drop and bubble break-up in turbulent dispersions. *Chem. Eng. Sci.* 64, 3389–3406.
- Liao, Y., Lucas, D., 2010. A literature review on mechanisms and models for the coalescence process of fluid particles. *Chem. Eng. Sci.* 65, 2851–2864.
- Liao, Y., Rzehak, R., Lucas, D., Krepper, E., 2015. Baseline closure model for dispersed bubbly flow: bubble coalescence and breakup. *Chem. Eng. Sci.* 122, 336–349.
- Luo, H., Svendsen, H.F., 1996. Theoretical model for drop and bubble break-up in turbulent dispersions. *AIChE J.* 42, 1225–1233.
- Machon, V., Pacek, A.W., Nienow, A.W., 1997. Bubble size in electrolyte and alcohol solutions in a turbulent stirred vessel. *Trans. Inst. Chem. Eng.* 75, 339–348.
- Marcelija, S., 2006. Selective coalescence of bubbles in simple electrolytes. *J. Phys. Chem. B* 110, 13062–13067.
- Marchisio, D.L., Fox, R.O., 2005. Solution of population balance equations using the direct quadrature method of moments. *Aerosol Sci.* 36, 43–73.
- Marrucci, G., Nicodemo, L., 1967. Coalescence of gas bubble in aqueous solutions in inorganic electrolytes. *Chem. Eng. Sci.* 22, 1257–1265.
- Marrucci, G., 1969. A theory of coalescence. *Chem. Eng. Sci.* 24, 975–985.
- Martinez-Bazan, C., Montanes, J.L., Lasheras, J.C., 1999. On the break-up of an air bubble injected into a fully developed turbulent flow. Part I. Break-up frequency. *J. Fluid Mech.* 401, 157–182.
- Martinez-Bazan, C., Rodriguez-Rodriguez, J., Deane, G.B., Montanes, J.L., Lasheras, J.C., 2010. Considerations on bubble fragmentation models. *J. Fluid Mech.* 661, 159–177.
- McGraw, R., 1997. Description of Aerosol dynamics by the quadrature method of moments. *Aerosol Sci. Tech.* 27, 255–265.
- Nasset, J.E., Finch, J.A., Gomez, C.O., 2007. Operating variables affecting the bubble size in forced air mechanical flotation machines. In: *Ninth Mill Operators' Conference 2007*. Australian Institute of Mining & Metallurgy, Fremantle, Western Australia, pp. 55–65.
- Omelka, B., Schreithofer, N., Wierink, G., Heiskanen, K., 2009. Particle detachment in flotation. In: *Proc. VI Int. Min. Proc. Semin., Santiago*, pp. 257–262.
- Prince, M.J., Blanch, H.W., 1990a. Bubble coalescence and break-up in air-sparged bubble columns. *AIChE J.* 36, 1485–1499.
- Prince, M.J., Blanch, H.W., 1990b. Transition electrolyte concentrations for bubble coalescence. *AIChE J.* 36, 1425–1429.
- Sagert, N.H., Quinn, M.J., Cribbs, S.C., Rosinger, L.J., 1976. Bubble coalescence in aqueous solutions of n-alcohols. In: *Akers, R.R. (Ed.), Foams*. Academic Press, Inc., New York, pp. 147–162.
- Solsvik, J., Jakobsen, H.A., 2015. Single air bubble break-up experiments in stirred water tank. *Int. J. Chem. React. Eng.* 10, 1–15.
- Stone, H.A., Leal, L.G., 1990. The effect of surfactants on drop deformation and breakage. *J. Fluid. Mech.* 220, 161–186.
- Sutherland, K.L., 1948. Physical chemistry of flotation IX. Kinetics of the flotation process. *J. Phys. Chem.* 52 (2), 394–425.
- Wang, T., Wang, J., Jin, Y., 2003. A novel theoretical break-up kernel function for bubbles/droplets in at turbulent flow. *Chem. Eng. Sci.* 58, 4629–4637.
- Yaminsky, V.V., Ohnishi, S., Vogler, E.A., Horn, R.G., 2010. Stability of aqueous films between bubbles. Part 1. The Effect of speed on bubble coalescence in purified water and simple electrolyte solutions. *Langmuir* 26 (11), 8061–8074.
- Yoon, R.-H., Luttrell, G.H., 1989. The effect of bubble size on fine particle flotation. *Min. Process Extr. Metall. Rev.* 5 (1&4), 101–122.
- Zhao, H., Ge, W., 2007. A theoretical bubble break-up model for slurry beds or three-phase fluidized beds under high pressure. *Chem. Eng. Sci.* 62, 109–115.